

# Palaeomagnetism of the ejecta-bearing Bunyerroo Formation, late Neoproterozoic, Adelaide fold belt, and the age of the Acraman impact

Phillip W. Schmidt<sup>a,1</sup>, George E. Williams<sup>b,\*</sup>

<sup>a</sup> CSIRO Division of Exploration and Mining, PO Box 136, North Ryde, NSW 2113, Australia

<sup>b</sup> Department of Geology and Geophysics, University of Adelaide, Adelaide, SA 5005, Australia

Received 9 February 1996; accepted 28 August 1996

---

## Abstract

A new palaeomagnetic study has been conducted on haematitic shales and siltstones of the late Neoproterozoic Bunyerroo Formation in the Adelaide fold belt (Geosyncline), South Australia, which host an extensive horizon of shock-deformed rock fragments and microtektite-like material of probable impact origin. Thermal step demagnetisation of 116 samples of red shale and siltstone from six sections (sites) revealed a high-temperature component with a bedding-corrected site-mean direction of remanence of  $D = 56.6^\circ$ ,  $I = 29.3^\circ$  ( $\alpha_{95} = 10.7^\circ$ ) that gives a pole at  $18.1^\circ\text{S}$ ,  $16.3^\circ\text{E}$  ( $dp = 6.5^\circ$ ,  $dm = 11.8^\circ$ ). The high-temperature component provides a positive tectonic-fold test (99% level of confidence). The Bunyerroo high-temperature remanence direction is near the remanence direction ( $D = 50^\circ$ ,  $I = 40^\circ$ ) indicated by modelling the subsurface magnetic source of the central high-amplitude anomaly at Acraman, Australia's largest confirmed meteorite impact structure 220–350 km west of the Adelaide fold belt, and also is close to the mean direction ( $D = 48.3^\circ$ ,  $I = 54.7^\circ$ ,  $\alpha_{95} = 5.2^\circ$ ) determined for surface melt rock from Acraman. Statistical tests show that the virtual geomagnetic poles indicated by the directions for the subsurface central magnetic source and surface melt rock at Acraman may be regarded as subsets of the Bunyerroo palaeomagnetic pole position, indicating that the three pole positions are statistically indistinguishable. The results imply that the subsurface magnetic source and surface melt rock acquired their remanence in the ambient geomagnetic field during cooling, after the impact when structural disturbance had ceased, while the Bunyerroo Formation was accumulating. The agreement among the various remanence directions argues strongly that the ejecta horizon in the Bunyerroo Formation was derived from Acraman.

The present findings confirm that the Acraman impact occurred in the late Neoproterozoic, about 590 Ma, which is the age of the Bunyerroo Formation provided by Rb–Sr whole-rock shale dating of equivalent and contiguous strata in the Adelaide fold belt region. The Bunyerroo palaeomagnetic data give a palaeolatitude of  $\sim 15^\circ$ , indicating a low palaeolatitude for the Acraman impact and supporting other findings that the Adelaide fold belt occupied low to equatorial palaeolatitudes during the late Neoproterozoic.

**Keywords:** impact features; ejecta; paleomagnetism; magnetic surveys

---

\* Corresponding author. Fax: +61 8 8303 5843. E-mail: gwilliams@geology.adelaide.edu.au

<sup>1</sup> E-mail: Phil.Schmidt@syd.dem.csiro.au.

## 1. Introduction

This study continues our work on the palaeomagnetism and deposition of late Neoproterozoic strata in the Adelaide fold belt (Adelaide Geosyncline), South Australia (Fig. 1). Here we present the results of a palaeomagnetic investigation of the Bunyeroo Formation (Fig. 2), a 400 m thick unit of mostly red shales and siltstones which hosts an extensive impact ejecta horizon up to 40 cm in thickness, located 80 m above the base of the formation. The ejecta horizon is marked by shock-deformed fragments of felsic volcanics, devitrified microtektite-like and shard-like material, and anomalous values for cosmogenic siderophile elements, including Ir [1–7]. We also examine the magnetic signature and palaeomagnetism of Acraman, Australia's largest confirmed meteorite impact structure, located 220–350 km west of the Adelaide fold belt [10–13], to test whether the Acraman impact and deposition of the Bunyeroo

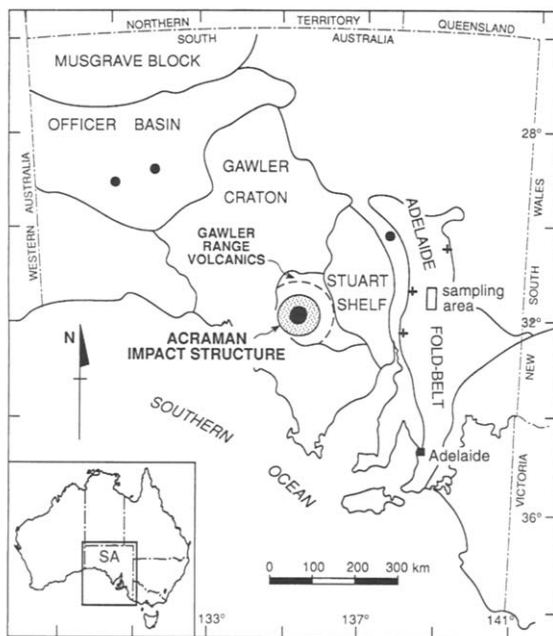


Fig. 1. Map of South Australia showing the sampling area for the Bunyeroo Formation in the Adelaide fold belt, the Acraman impact structure on the Gawler Craton, and the main localities of the ejecta horizon in the Adelaide fold belt and Officer Basin. Crosses = ejecta recorded in outcrop of the Bunyeroo Formation; small dots = ejecta in core from drill holes in the Bunyeroo Formation and equivalent strata in the Officer Basin (see [1,4,7]).

	STUART SHELF	CENTRAL FLINDERS ZONE	
WILPENA GROUP		Rawnsley Quartzite	MARINOAN
		Bonney Sandstone	
		Wonoka Formation	
	Yarloo Shale	Bunyeroo Formation	
	Tent Hill Formation	ABC Range Quartzite	
		Brachina Formation	
	Nuccaleena Formation	Nuccaleena Formation	
UMBERATANA GROUP	Whyalla Sandstone	Elatina Formation	STURTIAN
	"Yudnapinna Beds"	Trezona Formation	
		Enorama Shale	
		Etina Formation	
	Tapley Hill	Tapley Hill Formation	
	Woocalla Dolomite Member Formation		
	Sturt Tillite	Wilyerpa Formation	Merinjina Tillite

Fig. 2. Simplified stratigraphy of the late Neoproterozoic Umberatana and Wilpena groups of the Adelaide fold belt (Central Flinders Zone) and Stuart Shelf. Formations containing tillite are shown by solid triangles. HI = Holowilena Ironstone. The Wilpena Group is disconformably overlain by Early Cambrian strata (see [8,9]).

ejecta were contemporaneous and to establish the age of the impact.

Acraman lies almost entirely within the Yardea Dacite of the Gawler Range Volcanics, a Mesoproterozoic ( $1592 \pm 2$  Ma) continental suite of flat-lying, mainly felsic lavas and ash flows of the Gawler Craton [14,15]. Acraman displays numerous criteria for the identification of terrestrial impact structures: circular plan, concentric structure, negative gravity anomaly, magnetic low with subdued magnetic signature and central high-amplitude anomaly, shocked central area, intense brecciation and reduced magnetic susceptibility of bedrock, shatter cones in bedrock, multiple sets of planar shock lamellae in quartz grains in shattered bedrock, and the presence of melt rock [12,13,16]. Prior to deep erosion, Acraman evidently was a complex crater with a central peak. Suggested original diameters of major structural features at Acraman are  $\sim 20$  km for the extent of the 'peak ring' and central uplift,  $\sim 40$  km for the transient cavity/excavated area underlain by disrupted bedrock, 85–90 km for the possible final structural rim of the collapse crater, and  $\sim 150$  km

for arcuate lineaments at the outer limit of structural disturbance beyond the collapse crater.

Palaeomagnetic data for the Bunyeroo Formation [17] and for melt rock outcrop at the centre of Acraman [18] tentatively support correlation of the Acraman impact and deposition of the ejecta horizon in the Bunyeroo Formation. However, the timing of remanence in the Bunyeroo Formation was not unequivocally established by McWilliams and McElhinny [17], and palaeomagnetic data for Acraman are restricted to eight samples from a limited outcrop of melt rock. Here we provide new palaeomagnetic data for the Bunyeroo Formation, including a positive tectonic-fold test, and model the remanence direction for the magnetic source of the central high-amplitude anomaly at Acraman. The new data confirm our earlier conclusion [18] that the ejecta horizon in the Bunyeroo Formation was derived from Acraman.

## 2. Palaeomagnetism of the Bunyeroo Formation

The Bunyeroo Formation comprises mainly greyish to moderate red (5 R 5/2, 4/2, 4/4; colour designations from the Geological Society of America Rock-Color Chart, 1963) shale and siltstone of subtidal to marine-shelf origin [8]. Samples assayed 3.30–6.51% Fe<sub>2</sub>O<sub>3</sub> and 0.93–1.17% FeO, most of the iron being contained in a fine grained haematitic pigment.

An intermediate temperature (560°C) remanence direction ( $D = 66^\circ$ ,  $I = 40^\circ$ ,  $\alpha_{95} = 12^\circ$ ) determined previously for the Bunyeroo Formation [17] gives a pole at 7°S, 17°E ( $dp = 9^\circ$ ,  $dm = 14^\circ$ ). McWilliams and McElhinny [17] discussed the implications of the 50° difference in the pole positions between their results for the Bunyeroo Formation and for the underlying Brachina Formation (Fig. 2). Their favoured interpretation was that the Bunyeroo Formation was remagnetised during the Middle to Late Cambrian, albeit before folding of strata in the Adelaide fold belt during the Cambro–Ordovician Delamerian Orogeny. However, McWilliams and McElhinny [17] also included the Bunyeroo Formation pole in a table of possible primary pole positions, illustrating their uncertainty as to the timing of remanence. Unfortunately, the fold test applied to the Bunyeroo Formation by McWilliams and McElhinny [17] suffered from too little variation in structural attitudes to

Table 1  
Bunyeroo Formation sampling sites in the Adelaide fold belt

Site	Location		Bedding	
	Lat. (S)	Long. (E)	DDA (°)	Dip (°)
01	31°23'	138°35'	290	48
02	31°39'	138°36'	030	40
03	31°38'	138°35'	030	40
04	31°38'	138°35'	030	40
05	31°40'	138°41'	170	60
06	31°39'	138°43'	170	60

DDA = down-dip azimuth.

provide results at a sufficiently high level of confidence (95%).

### 2.1. Sampling

The present study of the Bunyeroo Formation has overcome the above-mentioned deficiency in structural attitudes by sampling fold limbs with steep dips (up to 60°) and strikes at large angles to the remanence directions. Using the results from McWilliams [19] as a guide, six sections (sites) were chosen to give a range of bedding attitudes that would allow unambiguous differentiation between pre- and post-folding remanence components. Table 1 lists both the locations and the bedding attitudes of the sections.

The Bunyeroo Formation was sampled within and immediately south of the Central Flinders Zone [8] west of longitude 139°00'E, to avoid the effects of slaty cleavage related to the Delamerian Orogeny. The Central Flinders Zone is the least deformed province of the Adelaide fold belt, and strata in this region display no obvious sign of metamorphism. At each section, between 10 and 29 samples were taken, up to 1 m apart stratigraphically. Taken together, the six sections span the whole Bunyeroo Formation, and include beds stratigraphically below and above the impact ejecta horizon.

### 2.2. Methods and techniques

Routine palaeomagnetic methods [20,21] were used throughout. Most samples were drilled in the field and oriented with both a magnetic and a sun

compass. Remanent magnetisations were measured using a CTF three-axis cryogenic magnetometer interfaced to a computer. The demagnetisers used were a Schonstedt AF demagnetiser model GSD-1 and the CSIRO automated three-stage carousel furnace. The furnace is housed inside a 4 m ten-coil Helmholtz set with automatic feed-back maintaining zero-field ( $< 5$  nT). All samples were subjected to thermal step demagnetisation, although some samples also were subjected to alternating field (AF) step demagnetisation. Components of magnetisation were isolated using an interactive version of LINEFIND [22], by which the linear segments are fitted to data points weighted according to the inverse of their measured variances.

### 2.3. Results

Natural remanent magnetisation (NRM) directions of the Bunyeroo Formation samples are spread from southwest to northeast of the dipole direction for the locality, with a mean declination of  $343.8^\circ$  and mean inclination of  $-59.4^\circ$ . The dipole declination is  $0.0^\circ$ , by definition, and the dipole inclination is  $-50.9^\circ$ , whereas the present field has a declination of  $7.4^\circ\text{E}$  and an inclination of  $-64.0^\circ$ , the latter being calculated from the 1995 Australian Geomagnetic Reference Field (Australian Geological Survey Organisation). It is apparent that the NRMs contain large components of present field and recent viscous remanent magnetisations (VRM). Intensities of NRM were typically  $2\text{--}10\text{ mA m}^{-1}$ , with a mean of  $5.1 \pm 3.2\text{ mA m}^{-1}$ . Nevertheless, the distribution of NRM directions southwest and northeast of the present/recent field direction suggests that there are relicts of normal and reverse ancient components as well.

Thermal step demagnetisation was found to be the most effective method to resolve the magnetic components present in the Bunyeroo Formation. During such demagnetisation, directions in many samples changed rapidly up to about  $600^\circ\text{C}$ , corresponding to the removal of secondary components, mainly northerly upward-directed and therefore interpreted as of recent origin (Fig. 3). The components remaining above  $600^\circ\text{C}$  changed little until above  $660^\circ\text{C}$ . Between  $660^\circ$  and  $690^\circ\text{C}$  the intensities decayed rapidly to the origin, yielding well defined single component high-temperature magnetisations. The in-

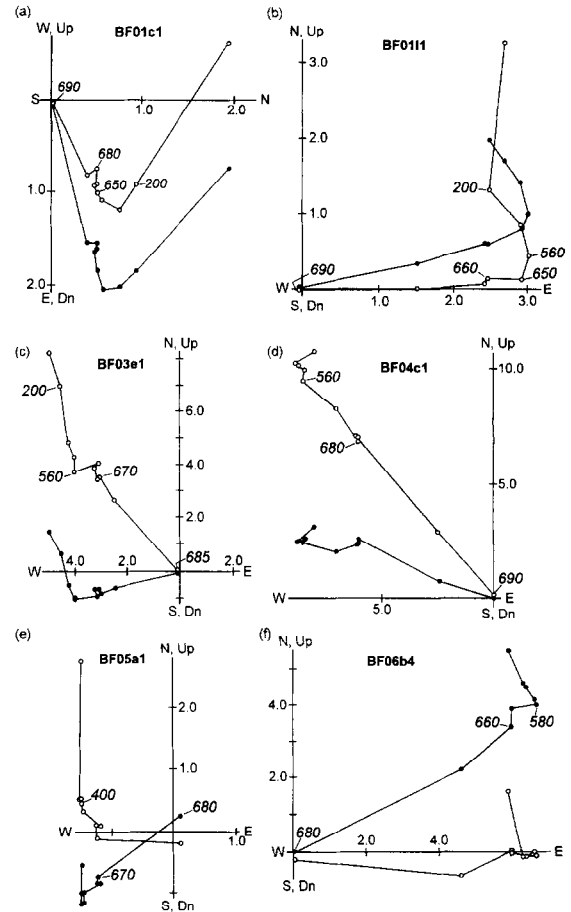


Fig. 3. Orthogonal projections showing examples of behaviour on thermal step demagnetisation of specimens of the Bunyeroo Formation. Dots = magnetisation vectors projected onto the horizontal plane; circles = projections onto the vertical plane. Units are  $\text{mA m}^{-1}$  ( $= 1\ \mu\text{G} = 10^{-6}\text{ emu/cc}$ ). The values plotted in italics next to data points refer to temperature ( $^\circ\text{C}$ ). Dn = down. (a) BF01c1 (site/sample/specimen). (b) BF0111. (c) BF03e1. (d) BF04c1. (e) BF05a1. (f) BF06b4.

ferred Curie temperature of about  $685^\circ\text{C}$  suggests that haematite is the remanence carrier. The Bunyeroo Formation appears to be consistent with the 'Type A red bed' classification of Turner [23], for which the mineralogy at the time of deposition is fairly mature and remanence is an early chemical remanent magnetisation (CRM).

Two components of remanence, therefore, are identified in the Bunyeroo Formation: a high-temperature component with a discrete unblocking temperature range above  $660^\circ\text{C}$ , and a component with

distributed unblocking temperatures that evidently has been recently acquired. The high-temperature component is scattered with respect to the present horizontal (Fig. 4a) but condenses into two anti-parallel groups after correction for bedding tilt (Fig. 4b).

Table 2 lists the high-temperature in situ mean site directions, the in situ and bedding-corrected site mean directions, and the bedding-corrected mean direction derived from the sample results. Following bedding-correction of high-temperature components for our new data, the sample (Fig. 4) and site mean directions become much more clustered and the precision parameter ( $k$ ) increases greatly (Table 2). The findings provide very strong evidence for pre-folding magnetisation using McFadden's [24] fold test (definition 1, since the in situ and bedding-corrected mean directions are similar; Table 2). The statistic  $\xi_1 = 5.826$  in situ, indicating that a high correlation

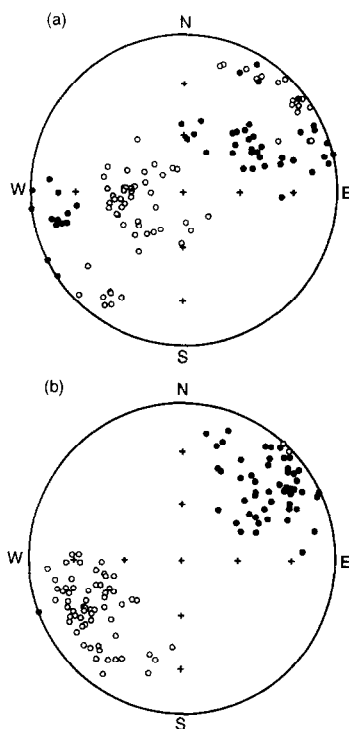


Fig. 4. Equal-area stereographic projections of the high-temperature magnetisation component directions isolated for samples from the Bunyeroo Formation using LINEFIND. (a) In situ directions. (b) Bedding-corrected directions. Dots = the lower hemisphere; circles = the upper hemisphere.

Table 2

Bunyeroo Formation high-temperature ( $> 650^{\circ}\text{C}$ ) in situ mean site directions for oriented samples, in situ and bedding-corrected site mean directions, and bedding-corrected sample mean direction, Adelaide fold belt

Site	N	D ( $^{\circ}$ )	I ( $^{\circ}$ )	k	$\alpha_{95}$ ( $^{\circ}$ )
01	21	69.8	34.7	21.9	6.9
02	22	38.5	23.1	14.5	8.4
03	15	57.3	22.0	35.7	6.5
04	29	51.8	24.2	14.9	7.2
05	10	72.3	39.1	33.0	8.5
06	19	53.7	29.3	18.7	8.0
Site mean (in situ)	6	60.4	28.7	4.88	33.8
Site mean <sup>a</sup>	6	56.6	29.3	40.4	10.7
Sample mean <sup>b</sup>	116	54.9	28.2	14.5	3.6

<sup>a</sup> Bedding-corrected; see Table 1 for structure at sites. Palaeomagnetic pole: latitude =  $18.1^{\circ}\text{S}$ , longitude =  $16.3^{\circ}\text{E}$  ( $dp = 6.5$ ,  $dm = 11.8$ ).

<sup>b</sup> Bedding-corrected; see Table 1 for structure at sites. Palaeomagnetic pole: latitude =  $19.8^{\circ}\text{S}$ , longitude =  $15.7^{\circ}\text{E}$  ( $dp = 2.2$ ,  $dm = 3.9$ ).

N = number of samples and sites; D = mean declination; I = mean inclination; k = precision parameter;  $\alpha_{95}$  = semi-angle of cone of 95% confidence about mean direction; dp and dm = semi-major and semi-minor axes of polar confidence oval ( $^{\circ}$ ).

exists between bedding structure and directional dispersion from the mean (the 99% critical point = 3.919). After correcting for bedding,  $\xi_1 = 2.650$ , which is less than the 95% critical point of 2.862, indicating that at this confidence level any correlation between bedding and directional dispersion no longer exists and that the remanence was most likely acquired before folding. The minimum  $\xi_1$  and maximum k occur at 83% and 85% unfolding, respectively, although the increase in k over the value after complete unfolding is not significant ( $53.2/40.4 = 1.32$ , cf.  $F(10,10) = 2.97$  [25]). Hence, there is no reason to suspect syn-folding magnetisation.

The stable, high-temperature component has a bedding-corrected site-mean declination of  $56.6^{\circ}$  and inclination of  $29.3^{\circ}$  ( $\alpha_{95} = 10.7^{\circ}$ ), yielding a palaeomagnetic pole at  $18.1^{\circ}\text{S}$ ,  $16.3^{\circ}\text{E}$  ( $dp = 6.5^{\circ}$ ,  $dm = 11.8^{\circ}$ ). For completion, it is of interest to compare this result with that of McWilliams and McElhinny [17], from whose data we have calculated a value for k of 19.9, compared with a value of 40.4 found here (Table 2). As expected, since the studies were of the same rock formation, the k values are not signifi-

cantly different ( $40.4/19.9 = 2.03$ , cf.  $F(16, 10) = 2.49$ ), and the appropriate test to apply is equation 29 of McFadden and Lowes [25]. The test statistic is 0.176, which is less than the 95% confidence critical value of 0.259, indicating that there is no significant difference between the bedding-corrected result of McWilliams and McElhinny [17] and that reported here. It is important to emphasise, however, that the present work has shown beyond doubt that the high-temperature remanence for the Bunyerroo Formation was acquired prior to folding.

### 3. Palaeomagnetism of melt rock from Acraman

Surface samples of melt rock from the centre of Acraman carried a remanent magnetisation that was stable to 630°C [18]. This observation, the coercivity of remanence, and X-ray diffraction and microprobe analyses indicate that the magnetic carrier is partially oxidised titanomagnetite. That carrier is likely to

have retained an original magnetic direction from the time of the impact.

The directions of the high-temperature components from eight prepared specimens of melt rock, and their mean direction ( $D = 48.3^\circ$ ,  $I = 54.7^\circ$ ,  $\alpha_{95} = 5.2^\circ$ ) give a mean pole position at  $8.6^\circ\text{S}$ ,  $353.4^\circ\text{E}$  ( $dp = 5.2^\circ$ ,  $dm = 7.4^\circ$ ). No dip correction has been made to the melt rock direction, because the Yardea Dacite is essentially flat-lying. The character of the remanence, such as low directional dispersion and high stability, is similar to that displayed by impactites containing melt material from other impact structures [26–28].

The direction of magnetisation of the melt rock is unlike the palaeomagnetic direction found in the Gawler Range Volcanics (see [29]). Furthermore, there is no sign of a present field direction attributable to weathering, or viscous remanent magnetisation (although a lightning-induced component may have obliterated the latter). It was thus concluded that the high-temperature component of the



Fig. 5. Aeromagnetic image of the central part of the Acraman structure, showing a circular magnetic low  $\sim 20$  km in diameter and a central high-amplitude dipolar anomaly. The east–west and north–south lines mark the positions of two profiles that pass through the central anomaly and which are modelled in Fig. 6. ER Mapper file: total magnetic intensity, greyscale, edges sharpened. Scale bar 10 km, north to top of image. Aeromagnetic data provided by MESA; see text for details of the aeromagnetic survey.

magnetisation dates from the time of cooling, immediately after the impact. However, the pole indicated for the melt rock must be considered a virtual geomagnetic pole (VGP) because the geomagnetic field direction recorded at the time of cooling is an instantaneous sample of a geomagnetic field direction subject to secular variation.

#### 4. Modelling of the central magnetic anomaly at Acraman

High-resolution digital aeromagnetic data for the Gawler Craton was released by Mines and Energy South Australia (MESA) in 1993 as part of the South Australian Exploration Initiative [9,30]. The surveys were flown at a constant 400 m line spacing along designated northings and eastings; the altitude specification was  $80 \pm 20$  m continuous ground clearance but the typical standard deviation of ground clearance attained was  $\pm 5$  m [31]. The data for Acraman reveal a conspicuous circular magnetic low  $\sim 20$  km in diameter exhibiting subdued magnetic relief and a central high-amplitude dipolar anomaly (Fig. 5). Specimens of shattered dacite from Acraman show a

70% decrease in magnetic susceptibility, on average, compared with specimens of undisturbed dacite, suggesting that the subdued magnetic signature at Acraman reflects a decrease in susceptibility.

The most common magnetic signature associated with impact structures is a magnetic low with subdued magnetic relief, caused by a reduction in susceptibility [32]. The presence at Acraman of a circular magnetic low, together with a reduced magnetic susceptibility of the shattered dacite, therefore strongly support an impact origin. The central high-amplitude dipolar anomaly equates with the central high-amplitude magnetic anomalies displayed by many impact structures, including all those  $> 40$  km in diameter (see [32]). The  $\sim 20$  km diameter circular magnetic low may mark the extent of the ‘peak ring’ and central uplift [16]; similarly, the  $\sim 50$  km diameter circular magnetic feature at the severely eroded 2000 Ma Vredefort impact structure in South Africa is much smaller than the estimated original crater diameter of  $\sim 300$  km (see [33]). The conspicuous regional magnetic signature for Acraman — one of the clearest recognised for a terrestrial impact structure — is attributable to the high quality of the aeromagnetic data and its occurrence in a thick and

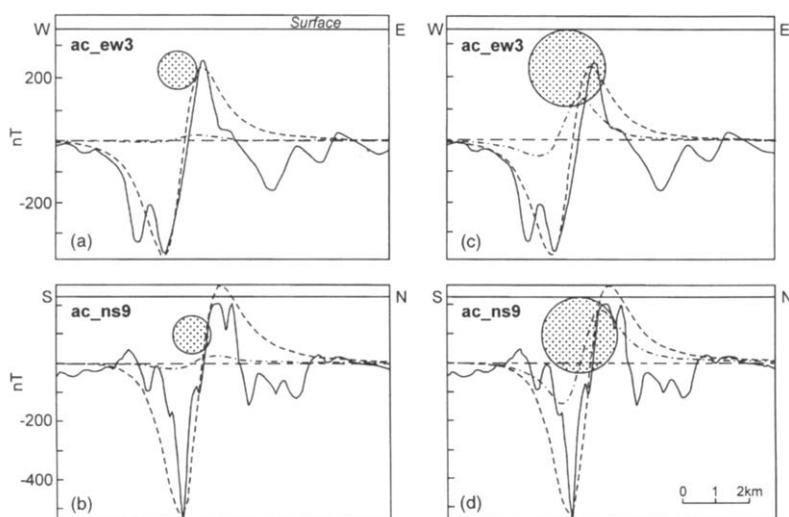


Fig. 6. Two sets of modelled profiles oriented east–west (ac\_ew3) and north–south (ac\_ns9) and passing through the central dipolar anomaly at Acraman (see Fig. 5). Continuous curves represent the observed anomalies, dashed curves represent best-fit profiles, and dot dash curves represent profiles calculated from measured properties of surface samples of melt rock. The source bodies’ centres are 1167 m deep, with diameters of 1167 m (a and b) and 2334 m (c and d). The Earth’s field, taken from the Australian Geological Survey Organisation’s Australian Geomagnetic Reference Field, has intensity =  $46 \text{ A/m}$  ( $0.58 \text{ Oe}$ ), declination =  $7^\circ$  and inclination =  $-64^\circ$ .

extensive body of flat-lying and homogeneous volcanics.

The central high-amplitude dipolar anomaly has an amplitude of about  $+300/-500$  nT and indicates a shallow magnetic source [16]. Two observed profiles oriented east–west and north–south and passing through the anomaly (Fig. 5) were selected for modelling. A spherical body magnetised by both induction and remanence yields a satisfactory fit to the main part of the anomaly, notwithstanding the ambiguity between ellipsoidal shapes and depths and the higher spacial frequencies present in the magnetic record, which we assume indicate shallow irregular sources in addition to the main body. This keeps the modelling as simple as possible, because we are fitting only four parameters: depth and radius of the sphere, and magnitudes of the susceptibility and remanence. The direction of the remanence is constrained, somewhat, by direct measurements on outcrop samples of melt rock [18], although the magnetic properties estimated from measurements of the melt rock samples are too feeble to explain the observed anomaly. Remanence of outcrop samples is commonly affected by weathering and/or lightning and, whereas palaeomagnetic cleaning can isolate the original remanence direction, the remanence magnitude is often irretrievable [34].

In model 1 (Fig. 6a,b), a sphere 1167 m in diameter and centred at a depth of 1167 m was taken as the source body, together with estimated values (based on measurements) for the following properties: susceptibility = 0.013 SI (0.001 cgs), natural remanent intensity = 0.5 A/m (500  $\mu$ cgs), declination =  $50^\circ$ , inclination =  $55^\circ$ . The estimated Koenigsberger ratio is therefore 0.86. The magnetic anomaly arising from these estimated values is more than an order of magnitude smaller than that observed. Although magnetic properties an order of magnitude greater than the estimated values yield a magnetic anomaly of the required magnitude, anomalies of higher frequency in the record suggest that a sphere is a crude representation of the source body. The high-frequency anomalies superimposed on the main, deeper body may be apophyses or dykes radiating from the top of the body.

The tenfold discrepancy between the estimated values and those demanded by model 1 can be reconciled, or at least ameliorated, by increasing the

volume of the body. This has been done in model 2 (Fig. 6c,d), in which the diameter has been doubled to 2334 m, so that the body just reaches the surface. The anomaly arising from the estimated values is clearly enhanced, but again is insufficient to adequately explain the observed anomaly. The form of the anomaly also is different, indicating that either a spherical source is incorrect or that the Koenigsberger ratio is incorrect. In the absence of further geological information, we explore here the implications of the latter suggestion, particularly since magnetic properties of surface samples are notoriously unrepresentative of the bulk properties at depth [34]. The best-fit values of properties are: susceptibility = 0.019 SI (0.0015 cgs), remanent intensity = 1.5 A/m (1500  $\mu$ cgs), declination =  $50^\circ$ , inclination =  $40^\circ$ . This implies a Koenigsberger ratio of 1.72. If we have approximated the volume of the source body accurately, the estimated values of properties for the surface samples of melt rock are significantly smaller than values for the bulk properties at depth. The susceptibility of the samples is lower by a factor of 2/3 and the remanent intensity is too low by a factor of three.

The results confirm that the magnetisation direction of the subsurface magnetic source is similar to that observed in the melt rock. The body indicated (or an ellipsoidal equivalent) may be quite large, possibly about 2 km in diameter and centred about 1 km below the surface. The anomaly may reflect basement rocks brought from great depth by structural uplift and remagnetised by the impact (shock remanent magnetisation, see [32]); or thermoremanent magnetisation, see [33]), or a concentration of impact-produced melt rock or melt-bearing breccia. The postulated large volume of the main magnetic source would seem to favour remagnetisation of basement, rather than a body of melt material. In the absence of outcrop, drilling will be required to determine the nature of the magnetic source.

## 5. Bunyeroo–Acraman palaeomagnetic correlation and age of the Acraman impact

The value of aeromagnetic and palaeomagnetic studies in determining the age of impact events has been demonstrated for several impact structures, in-



Table 3

Remanence directions for the Bunyeroo Formation in the Adelaide fold belt, and for surface melt rock and the subsurface central magnetic source at Acraman

	$D$ ( $^{\circ}$ )	$I$ ( $^{\circ}$ )	$\alpha_{95}$ ( $^{\circ}$ )
Bunyeroo Formation [17]	66	40	12
Bunyeroo Formation (this study)	54.9	28.2	3.6
Acraman melt rock [18]	48.3	54.7	5.2
Modelling of central magnetic source	50	40	–

Abbreviations and symbols as for Table 2.

cluding Gosses Bluff in central Australia [35,36], Manicouagan in Quebec [26,37], Rochechouart in France [28] and Lonar Lake in India [38]. Here we employ palaeomagnetic and aeromagnetic data to confirm a late Neoproterozoic age for Acraman in South Australia.

The mean directions of remanence for the Bunyeroo Formation ([17], and this study), Acraman melt rock, and the central high-amplitude dipolar anomaly at Acraman are summarised in Table 3 and plotted in Fig. 7. Statistical tests show that the melt rock VGP and the mean direction for the central anomaly may be regarded as subsets of the Bunyeroo palaeomagnetic pole position as determined here. The divergence of the measured melt rock remanence direction from the Bunyeroo Formation mean direction is  $26.1^{\circ}$  (from Table 3). Using the test of McFadden [39], in a random sampling of seven directions from the Bunyeroo Formation population (corresponding to six sites plus another), there is a 40% probability that the most divergent of these seven directions will fall beyond this angle. Similarly, the divergence of the modelled subsurface direction is  $12.0^{\circ}$ , which corresponds to a 99% probability of a greater angle being made by the most divergent of seven random directions. Consequently, there is no cause to suggest that the melt rock remanence, either as measured or as modelled, does not belong to the Bunyeroo Formation population.

The results imply that the melt rock and subsurface central magnetic source at Acraman acquired their magnetic remanence in the ambient geomagnetic field during cooling after the impact when structural disturbance had ceased, while the Bunyeroo Formation was accumulating. Such agreement

among magnetic directions argues forcibly that the ejecta horizon in the Bunyeroo Formation was derived from Acraman. Determination of the age of the Bunyeroo Formation, therefore, should provide the age of the Acraman impact. The Yarloo Shale, the equivalent of the Bunyeroo Formation on the Stuart Shelf (Fig. 2), gave a Rb–Sr whole-rock shale age of  $588 \pm 35$  Ma [40], and combined Rb–Sr whole-rock data for the Yarloo Shale and subjacent shales gave a mean age of  $593 \pm 32$  Ma [3]. Thus, the age of the Bunyeroo Formation and, by implication, the age of the Acraman impact event, may be approximated as 590 Ma. While recognising the potential shortcomings of Rb–Sr shale dating, this result accords with the stratigraphic position of the Bunyeroo Formation below the level of first appearance of Ediacaran megafauna at the top of the Wonoka Formation (Fig. 2; see [41]). A late Neoproterozoic age is consistent with the severe degradation of Acraman.

Conventional K/Ar and  $^{40}\text{Ar}/^{39}\text{Ar}$  total fusion and step heat experiments performed on samples of the melt rock [42] could not determine the true age of the impact, because the feldspars in the melt rock evidently formed as a result of low-temperature authigenic replacement and devitrification. Hence, the apparent age of 450 Ma obtained by these methods is regarded as a *minimum*, reflecting secondary processes rather than the impact event itself [12,13,42].

The Bunyeroo palaeomagnetic data (Table 2) in-

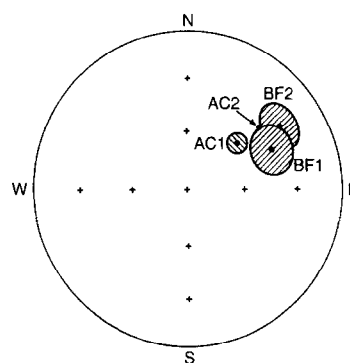


Fig. 7. Equal-area stereographic projections for bedding-corrected, high-temperature, mean magnetisation directions for the Bunyeroo Formation (BF1 [17]; BF2, this study), the high-temperature, mean magnetisation direction for Acraman melt rock (AC1 [18]), and the direction indicated by modelling the subsurface magnetic source of the central high-amplitude dipolar anomaly at Acraman (AC2).

dicating a palaeolatitude of  $15.7 \pm 6.5^\circ$  for site-mean results and  $15.0 \pm 2.2^\circ$  for sample-mean results (where palaeolatitude,  $\lambda$ , is provided by the dipole formula  $\tan I = 2 \tan \lambda$ , and the error limit by the magnitude of  $dp$ ), indicating that the Acraman impact occurred in low palaeolatitudes. The present study therefore provides strong support for previous findings [17,43–45] that the Adelaide fold belt occupied low to equatorial palaeolatitudes during the late Neoproterozoic.

## 6. Conclusions

This study continues our investigations of the palaeomagnetism and deposition of late Neoproterozoic strata in the Adelaide fold belt. The main conclusions are as follows:

(1) New palaeomagnetic data for red beds of the ejecta-bearing Bunyeroo Formation reveal a high-temperature component with a bedding-corrected site-mean direction of remanence of  $D = 56.6^\circ$ ,  $I = 29.3^\circ$  ( $\alpha_{95} = 10.7^\circ$ ) that gives a pole at  $18.1^\circ\text{S}$ ,  $16.3^\circ\text{E}$  ( $dp = 6.5^\circ$ ,  $dm = 11.8^\circ$ ). This component gives a positive tectonic-fold test at the 99% level of confidence.

(2) Modelling of the subsurface magnetic source of the central high-amplitude anomaly at Acraman, Australia's largest confirmed meteorite impact structure, 220–350 km west of the Adelaide fold belt, gives a remanence direction ( $D = 50^\circ$ ,  $I = 40^\circ$ ) that is near the Bunyeroo high-temperature direction and close to the mean direction ( $D = 48.3^\circ$ ,  $I = 54.7^\circ$ ,  $\alpha_{95} = 5.2^\circ$ ) determined for surface melt rock from Acraman.

(3) The virtual geomagnetic poles indicated by the directions for the subsurface central magnetic source and surface melt rock at Acraman are statistically indistinguishable from the Bunyeroo palaeomagnetic pole position. The results imply that the magnetic source and melt rock acquired their remanence in the ambient geomagnetic field during cooling after the impact, when structural disturbance had ceased, while the Bunyeroo Formation was accumulating. The agreement among the various remanence directions argues strongly that the Acraman impact was the source of the ejecta horizon in the Bunyeroo Formation.

(4) Our findings confirm that the Acraman impact

occurred in the late Neoproterozoic, about 590 Ma, which is the age of the Bunyeroo Formation given by Rb–Sr whole-rock shale dating.

(5) The Bunyeroo Formation was deposited at a palaeolatitude of  $\sim 15^\circ$ , indicating a low palaeolatitude for the Acraman impact and in agreement with other findings that the Adelaide fold belt occupied low to equatorial palaeolatitudes during the late Neoproterozoic.

## Acknowledgements

We thank Mines and Energy South Australia for providing the aeromagnetic data for Acraman, David Boyd and Dave Clark for discussion, and Robert B. Hargraves for a constructive review of the manuscript. Williams is supported by an Australian Research Council Senior Research Fellowship. [RV]

## References

- [1] V.A. Gostin, P.W. Haines, R.J.F. Jenkins, W. Compston and I.S. Williams, Impact ejecta horizon within late Precambrian shales, Adelaide Geosyncline, South Australia, *Science* 233, 198–200, 1986.
- [2] V.A. Gostin, R.R. Keays and M.W. Wallace, Iridium anomaly from the Acraman impact ejecta horizon: impacts can produce sedimentary iridium peaks, *Nature* 340, 542–544, 1989.
- [3] W. Compston, I.S. Williams, R.J.F. Jenkins, V.A. Gostin and P.W. Haines, Zircon age evidence for the Late Precambrian Acraman ejecta blanket, *Aust. J. Earth Sci.* 34, 435–445, 1987.
- [4] M.W. Wallace, V.A. Gostin and R.R. Keays, Discovery of the Acraman impact ejecta blanket in the Officer Basin and its stratigraphic significance, *Aust. J. Earth Sci.* 36, 585–587, 1989.
- [5] M.W. Wallace, G.E. Williams, V.A. Gostin and R.R. Keays, The Late Proterozoic Acraman impact — towards an understanding of impact events in the sedimentary record, *Mines Energy Rev. S. Aust.* 57, 29–35, 1990.
- [6] M.W. Wallace, V.A. Gostin and R.R. Keays, Acraman impact ejecta and host shales: evidence for low-temperature mobilization of iridium and other platinoids, *Geology* 18, 132–135, 1990.
- [7] M.W. Wallace, V.A. Gostin and R.R. Keays, Spherules and shard-like clasts from the late Proterozoic Acraman impact ejecta horizon, South Australia, *Meteoritics* 25, 161–165, 1990.
- [8] W.V. Preiss, compiler, The Adelaide Geosyncline, *Geol. Surv. S. Aust. Bull.* 53, 438 pp., 1987.
- [9] J.F. Drexel, W.V. Preiss and A.J. Parker, eds., The Geology of South Australia, Vol. 1, The Precambrian, *Geol. Surv. S. Aust. Bull.* 54, 242 pp., 1993.

- [10] G.E. Williams, The Acraman impact structure: source of ejecta in late Precambrian shales, South Australia, *Science* 233, 200–203, 1986.
- [11] G.E. Williams, The Acraman structure — Australia's largest impact scar, *Search* 18, 143–145, 1987.
- [12] G.E. Williams, Acraman: A major impact structure from the Neoproterozoic of Australia, in: *Large Meteorite Impacts and Planetary Evolution*, B.O. Dressler, R.A.F. Grieve and V.L. Sharpton, eds., *Geol. Soc. Am. Spec. Pap.* 293, 209–224, 1994.
- [13] G.E. Williams, Acraman, South Australia: Australia's largest meteorite impact structure, *Proc. R. Soc. Victoria* 106, 105–127, 1994.
- [14] C.M. Fanning, R.B. Flint, A.J. Parker, K.R. Ludwig and A.H. Blissett, Refined Proterozoic evolution of the Gawler Craton, South Australia, through U–Pb zircon geochronology, *Precambrian Res.* 40/41, 363–386, 1988.
- [15] R.A. Creaser and A.J.R. White, Yardea Dacite — large-volume, high-temperature felsic volcanism from the Middle Proterozoic of South Australia, *Geology* 19, 48–51, 1991.
- [16] G.E. Williams, P.W. Schmidt and D.M. Boyd, Magnetic signature and morphology of the Acraman impact structure, South Australia, *Aust. Geol. Surv. O. J. Geol. Geophys.* 16, 431–442, 1996.
- [17] M.O. McWilliams and M.W. McElhinny, Late Precambrian palaeomagnetism of Australia: the Adelaide Geosyncline, *J. Geol.* 88, 1–26, 1980.
- [18] P.W. Schmidt and G.E. Williams, Palaeomagnetic correlation of the Acraman impact structure and the Late Proterozoic Bunyeruo ejecta horizon, South Australia, *Aust. J. Earth Sci.* 38, 283–289, 1991.
- [19] M.O. McWilliams, Late Precambrian palaeomagnetism of Australia and Africa, Ph.D. Thesis, Australian National Univ., 62 pp., 1977.
- [20] D.W. Collinson, *Methods in Rock Magnetism and Palaeomagnetism*, 503 pp., Chapman and Hall, London, 1983.
- [21] R.F. Butler, *Paleomagnetism: Magnetic Domains to Geologic Terranes*, 319 pp., Blackwell, Oxford, 1992.
- [22] J.T. Kent, J.C. Briden and K.V. Mardia, Linear and planar structure in ordered multivariate data as applied to progressive demagnetization of palaeomagnetic remanence, *Geophys. J. R. Astron. Soc.* 75, 593–621, 1983.
- [23] P. Turner, *Continental Red Beds, Developments in Sedimentology* 29, 562 pp., Elsevier, Amsterdam, 1980.
- [24] P.L. McFadden, A new fold test for palaeomagnetic studies, *Geophys. J. Int.* 103, 163–169, 1990.
- [25] P.L. McFadden and F.J. Lowes, The discrimination of mean directions drawn from Fisher distributions, *Geophys. J. R. Astron. Soc.* 67, 19–33, 1981.
- [26] A. Laroche and K.L. Currie, Paleomagnetic study of igneous rocks from the Manicouagan structure, Quebec, *J. Geophys. Res.* 72, 4163–4169, 1967.
- [27] J. Pohl, On the origin of the magnetization of impact breccias on Earth, *Zeit. Geophys.* 37, 549–555, 1971.
- [28] J. Pohl and H. Soffel, Paleomagnetic age determination of the Rochechouart impact structure (France), *Zeit. Geophys.* 37, 857–866, 1971.
- [29] F.H. Chamalaun and C.E. Dempsey, Palaeomagnetism of the Gawler Range Volcanics and implications for the genesis of the Middleback hematite orebodies, *J. Geol. Soc. Aust.* 25, 255–265, 1978.
- [30] W.V. Preiss (ed.), *South Australian Resources, Technical Sessions Abstracts, Mines and Energy S. Australia*, Adelaide, 73 pp., 1993.
- [31] D.H. Tucker, Gawler Craton — airborne geophysics, in: *South Australian Resources, Technical Sessions Abstracts, W.V. Preiss, ed.*, pp. 6–11, Mines and Energy S. Australia, Adelaide, 1993.
- [32] M. Pilkington and R.A.F. Grieve, The geophysical signature of terrestrial impact structures, *Rev. Geophys.* 30, 161–181, 1992.
- [33] R.J. Hart, R.B. Hargraves, M.A.G. Andreoli, M. Tredoux and C.M. Doucouré, Magnetic anomaly near the center of the Vredefort structure: implications for impact-related magnetic signatures, *Geology* 23, 277–280, 1995.
- [34] D.A. Clark, Comments on magnetic petrophysics, *Bull. Aust. Soc. Explor. Geophys.* 14, 49–62, 1983.
- [35] D.J. Milton, B.C. Barlow, R. Brett, A.R. Brown, A.Y. Glikson, E.A. Manwaring, F.J. Moss, E.C.E. Sedmik, J. van Son and G.A. Young, Gosses Bluff impact structure, Australia, *Science* 175, 1199–1207, 1972.
- [36] P.W. Schmidt and B.J.J. Embleton, Magnetic overprinting in southeastern Australia and the thermal history of its rifted margin, *J. Geophys. Res.* 86, 3998–4008, 1981.
- [37] W.A. Robertson, Manicouagan, Quebec, paleomagnetic results, *Can. J. Earth Sci.* 4, 641–649, 1967.
- [38] G.V.S. Poornachandra Rao and M.S. Bhalla, Lonar Lake: palaeomagnetic evidence of shock origin, *Geophys. J. R. Astron. Soc.* 77, 847–862, 1984.
- [39] P.L. McFadden, Rejection of palaeomagnetic observations, *Earth Planet. Sci. Lett.* 61, 392–395, 1982.
- [40] A.W. Webb, R.P. Coats, C.M. Fanning and R.B. Flint, Geochronological framework of the Adelaide Geosyncline, *Geol. Soc. Aust. Abstr.* 10, 7–9, 1983.
- [41] R.J.F. Jenkins, Ediacaran events: boundary relationships and correlation of key sections, especially in "Armorica", *Geol. Mag.* 121, 635–643, 1984.
- [42] S.L. Baldwin, I. McDougall and G.E. Williams, K/Ar and <sup>40</sup>Ar/<sup>39</sup>Ar analyses of meltrock from the Acraman impact structure, Gawler Ranges, South Australia, *Aust. J. Earth Sci.* 38, 291–298, 1991.
- [43] B.J.J. Embleton and G.E. Williams, Low palaeolatitude of deposition for late Precambrian periglacial varvites in South Australia: implications for palaeoclimatology, *Earth Planet. Sci. Lett.* 79, 419–430, 1986.
- [44] P.W. Schmidt, G.E. Williams and B.J.J. Embleton, Low palaeolatitude of Late Proterozoic glaciation: early timing of remanence in haematite of the Elatina Formation, South Australia, *Earth Planet. Sci. Lett.* 105, 355–367, 1991.
- [45] P.W. Schmidt and G.E. Williams, The Neoproterozoic climatic paradox: Equatorial palaeolatitude for Marinoan glaciation near sea level in South Australia, *Earth Planet. Sci. Lett.* 134, 107–124, 1995.